## Geometry-dependent scattering through quantum billiards: Experiment and theory

T. Blomquist,<sup>1</sup> H. Schanze,<sup>2</sup> I. V. Zozoulenko,<sup>3,1</sup> and H.-J. Stöckmann<sup>2</sup>

<sup>1</sup>Department of Physics (IFM), Linköping University, S-58183 Linköping, Sweden

<sup>2</sup>Fachbereich Physik, Philipps-Universität Marburg D-35032 Marburg, Germany

<sup>3</sup> Department of Science and Technology (ITN),

Linköping University, S-60174 Norrköping, Sweden

(Dated: October 28, 2018)

We present experimental studies of the geometry-specific quantum scattering in microwave billiards of a given shape. We perform full quantum mechanical scattering calculations and find an excellent agreement with the experimental results. We also carry out the semiclassical calculations where the conductance is given as a sum of all classical trajectories between the leads, each of them carrying the quantum-mechanical phase. We unambiguously demonstrate that the characteristic frequencies of the oscillations in the transmission and reflection amplitudes are related to the length distribution of the classical trajectories between the leads, whereas the frequencies of the probabilities can be understood in terms of the length difference distribution in the pairs of classical trajectories. We also discuss the effect of non-classical "ghost" trajectories that include classically forbidden reflection off the lead mouths.

PACS numbers: 05.45.Mt, 03.65.Sq, 73.23.-b, 73.23.Ad

The low-temperature conductance of nanoscaled semiconductor quantum dots (often called quantum billiards) is dominated by quantum mechanical interference of electron waves giving rise to reproducible conductance oscillations [1, 2, 3, 4, 5, 6, 7, 8, 9, 10]. Theoretical and experimental studies of the conductance oscillations have been concentrated on both statistical and geometry-specific features [1, 2, 3, 4, 5, 6, 7, 8, 9, 10, 11, 12, 13, 14, 15, 16, 17]. The analysis of the statistical aspects of the conductance was commonly based on the random matrix theory or similar stochastic methods [12]. In order to provide the interpretation of the geometry-specific features in the oscillations in a billiard of a given shape, different and sometimes conflicting approaches have been used [1, 2, 3, 4, 5, 6, 7, 8, 9, 10, 11, 14, 15, 16, 17]. Very often the interpretation of the conductance was not directly based on the transport calculations such that the explanation of the characteristic peaks in the conductance spectrum had rather speculative character. In contrast, the semiclassical approach [13, 14, 15, 16, 17, 18, 19] represents one of the most powerful tool for studying the geometry-specific scattering as it allows one to perform transport calculations for structures of arbitrary geometry and, at the same time, it can provide an intuitive interpretation of the conductance in terms of classical trajectories connecting the leads, each of them carrying the quantum mechanical phase.

In this paper we, for the first time, present experimental studies of the geometry-specific quantum scattering in microwave billiards of a given shape combined with the exact quantum mechanical as well as semi-classical analysis. The physics and modelling of microwave cavities is conceptually similar to that one of the semiconductor quantum dots because of the similarity between the

Schrödinger and Helmholtz equations [19, 20]. At the same time, the microwave cavities provide the unique opportunity to control the precise shape of the billiard. This is not possible for the semiconductor quantum dots where the actual shape of the potential always remains unknown [21]. Secondly, for the microwave billiards one can routinely access the phase information (i.e. measuring the transmission and reflection amplitudes) whereas for the case of quantum dot one typically measures the transmission probabilities only. Thirdly, the effects of inelastic scattering is of much lesser importance for the microwave cavities than for the quantum dots where the phase breaking processes can reduce the phase coherence length significantly. Note that a billiard system of the same shape as the one studied here (realized as a semiconductor quantum dot), was investigated in [5, 16]. It has been demonstrated [16] that the strong inelastic scattering has lead to the suppression of major characteristic peaks in the transmission spectrum as well as to the strong reduction of the amplitude of the oscillations.

Our semiclassical (SC) analysis of the experimental spectrum of the microwave billiard unambiguously demonstrate that the characteristic frequencies of the oscillations in the transmission and reflection amplitudes are related to the length distribution of the classical trajectories between the leads, whereas the frequencies of the probabilities can be understood in terms of the length difference distribution in the pairs of classical trajectories. This, to the best of our knowledge, provides the first unambiguous identification of the specific frequencies of the oscillations experimentally observed in a billiard of a given shape.

The dynamics of an electron in a two-dimensional

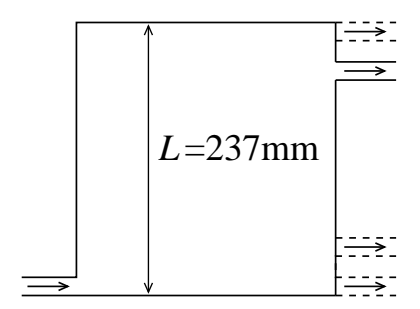


FIG. 1: Sketch of the resonator used in the experiment (in scale). Measurements have been taken for four different positions of the outgoing wave guide as indicated in the figure.

quantum dot is governed by the Schrödinger equation

$$\left(\frac{\hbar^2}{2m}\nabla^2 + E\right)\psi(x,y) = 0,\tag{1}$$

with the wave function vanishing on the boundary  $\psi = 0$ , where E is the electron Fermi energy and a potential inside the billiard is assumed to be zero. This equation has the same form as the Helmholtz equation governing the dynamics of the lowest TM-mode in a microwave billiards [19] (provided the frequency  $\nu < c/2d$ , where d is the heigt of the billiard).

In the absence of a magnetic field the transmission amplitude  $t_{nm}$  is given by the projection of the retarded Green function  $G = (H - E)^{-1}$  onto the transverse wave functions  $\phi_n(y)$  in the incoming and outgoing leads [22]

$$t_{mn}(k) = -i\hbar\sqrt{v_n v_m}$$

$$\times \int dy_1 \int dy_2 \phi_n^*(y_1) \phi_m(y_2) G(y_1, y_2, k),$$
(2)

where  $v_n$  is the longitudinal velocity for the mode n and k is the wave vector. The total transmission probability  $T = \sum_{mn} T_{mn}$  is the sum over transmission probabilities from all the propagating modes m in one lead to the modes n in the other;  $T_{mn}$  being the square modulus of the transmission amplitude,  $T_{mn} = |t_{mn}|^2$ .

The quantum mechanical computations have been made using a recursive Green's function technique based on the Dyson equation [23]. In semi-classical computations, the quantum mechanical Green's function is replaced by its semiclassical approximation [18, 19]. The semiclassical transmission amplitude can be represented in the form [14, 15, 16, 17]

$$t_{mn}^{SC}(k) = \sum_{s} A_{mn}^{s} e^{ikl_s}, \qquad (3)$$

where s denotes classical trajectories of the length  $l_s$  between the two leads,  $A_{mn}^s$  is an amplitude factor which depends on the density of trajectories, mode number, entrance and exit angles, etc. The details of the semiclassical calculations are given in [17].

Because of the rapidly varying phase factor in Eq. (3), the length spectrum of the transmission amplitude (defined as a Fourier Transform  $\int d\ell \ t_{mn}^{SC}(k)e^{-k\ell}$ ), is obviously peaked at the length  $\ell = l_s$  of the trajectories between the leads. This behavior of the length spectrum is well understood and numerically verified for a number of different model billiards with leads [14, 15, 16].

Using Eq. (3), the transmission probability can be written in the form

$$T_{mn}^{SC} = |t_{mn}^{SC}|^2 = \sum_{s} |A_{mn}^{s}|^2 + \sum_{s,s'} A_{mn}^{s} A_{mn}^{s'}^{*} e^{ik(l_s - l_{s'})}.$$
(4

The length spectrum of the transmission probability is obviously peaked at the length difference  $\ell = l_s - l_{s'}$  in the pairs of trajectories between the leads. Thus, identification of the characteristic frequencies in the probabilities reduces to the analysis of the path difference distribution in a billiard with a given lead geometry[14, 17].

Figure 1 shows a sketch of the microwave resonator used in the experiments. The microwaves enter the resonator through a wave guide at a fixed position on one side, and leaves the resonator through another waveguide on the opposite side whose position could be varied. The height of the resonator was d=7.8 mm, i.e. the billiard is quasi-two-dimensional for  $\nu<19$  GHz. Transmision spectra, including modulus and phase, were taken in the frequency range 10 to 18 GHz for four different positions of the outgoing wave guide. In the whole frequency range there is only one propagating mode in the wave guide. More details on the experimental technique may be found in [24].

Figure 2 shows the experimental and calculated data for the transmission and reflection amplitudes. The agreement between the experimental results and exact quantum mechanical (QM) calculations is very good. The SC transport calculations allows us to identify the characteristic peaks in the spectrum in terms of classical trajectories connecting the billiard leads. Indeed, each peak in the SC spectrum represents a contribution from a particular classical trajectory, as illustrated in the insets. However, because of the approximate nature of the semiclassical approximation, the heights of the SC and QM peaks do not fully agree with each other.

Furthermore, the experimental data as well as the QM calculations show the presence of the peaks which are absent in the SC calculations (for example, the peaks at  $l \approx 5.5, 9, 10.5$  in the reflection amplitude). These are so-called "ghost" trajectories that include classically forbidden reflection off the lead mouths [14]. For example, the peak in the reflection amplitude at  $l \approx 9$  is caused by the trajectory with the length l = 4.5 which, after one revolution in the billiard, is reflected back at the exit by the lead mouth such that it makes one more revolution and its total length becomes  $L = 4.5 \times 2 \approx 9$ . Such non-classical trajectories are not included in the standard

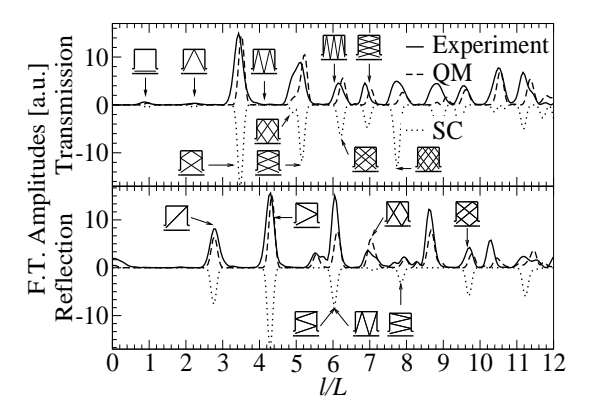


FIG. 2: Fourier transform of the experimental and calculated quantum mechanical (QM) transmission and reflection amplitudes for the square billiard with opposite leads. The lower curve shows corresponding semiclassical (SC) results, plotted with a negative sign for the sake of clearness. The characteristic peaks are identified in terms of classical transmitted and reflected trajectories. Peaks in the reflection amplitude at  $l\approx 5.5L$ , 8.8L are due to "ghost" trajectories that include classically forbidden reflection off the lead mouths. The range of the frequency variation corresponds to one propagating mode in the leads. The insets show the schematic geon

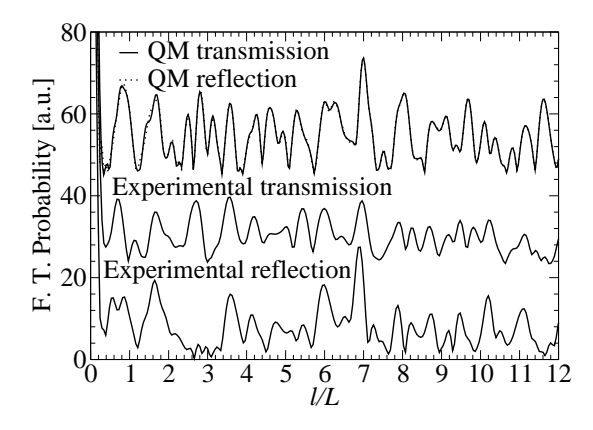


FIG. 3: Fourier transform of the experimental and calculated quantum mechanical (QM) transmission and reflection *probabilities* for the square billiard with opposite leads.

semiclassical approximation.

The "ghost" trajectories are more important for the reflection than for the transmission. This is due to the fact that each "ghost" trajectory manifesting itself in the reflection bounces off the lead mouth only once, whereas each "ghost" trajectory contributing to the transmission has to bounce off the lead mouth twice. As a result, the amplitude of such the trajectory with two non-classical bounces off the lead mouth is obviously lower than the one with only one bounce.

Experimental and calculated QM transmission and reflection *probabilities* are shown in Fig. 3. The correspondence between the theoretical and experimental probabilities is also rather good. Note that because of the

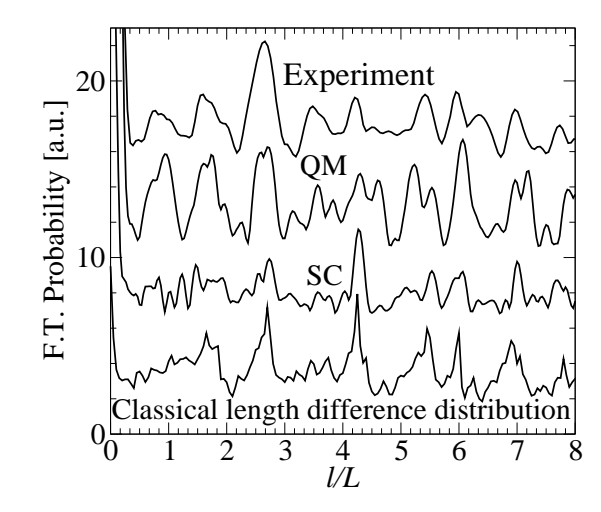


FIG. 4: Fourier transform of the experimental, quantum mechanical (QM) and semiclassical (SC) transmission probabilities in a square billiard averaged over four different lead positions. The characteristic frequencies in the transmission probabilities can be understood in terms of the length difference distribution in the pairs of classical trajectories between the leads (the lower curve).

current conservation requirement, R+T=1, the variation of the transmission is opposite to that one of the reflection,  $\delta T=-\delta R$ . As a result, the FT of the calculated QM transmission and reflection probabilities are practically identical. This is however not the case for the experimental transmission and reflection probabilities. This is because of the presence of some absorption in the system. As we do not include neither absorption nor inelastic scattering in the theoretical calculations, this is the reason for some discrepancy existing between the QM calculations and the experiment.

In contrast to the case of SC and QM amplitudes, the agreement between the SC and QM probabilities is only marginal (therefore we do not show the SC results here). Because the probabilities are the squared moduli of the amplitudes, the discrepancy which exists between the SC and QM amplitudes, see Fig. 2, becomes much more pronounced for the *probabilities* (a detailed analysis of the discrepancy between the SC and QM approaches is given in [17]). Furthermore, the interval of the frequency variation (limited to one propagating mode in the leads) is not wide enough to ensure reliable statistics for the probabilities. The calculations demonstrate that with a wider frequency interval the characteristic peaks in the FT spectrum become better resolved and the agreement between the QM and SC results improves significantly. Experimentally, however, it is not possible to access the frequency range beyond one propagating mode in the leads.

In order to provide the SC interpretation of the probabilities in the available frequency interval (limited to one propagating mode), we perform the averaging over

four different lead geometries, see Fig. 4. Such the averaging is justified because the characteristic frequencies of the oscillations in a square billiard are shown to be rather insensitive to the lead positions [16]. This, in turn, is related to the fact that classical length difference distribution is also not sensitive to the lead positions. The averaged QM probabilities show pronounced peaks in the FT which are in a good agreement with the corresponding experimental ones. The correspondence between the averaged QM and SC results is also rather good. According to the SC approach, the characteristic peaks in the SC spectra can be understood in terms of the length differences in pairs of classical trajectories connecting the leads, see Eq. (4). This is demonstrated in Fig. 4 where the experimental and calculated spectra are compared to the classical length difference distribution between the leads. This provides us with the semiclassical interpretation of the calculated QM (and therefore observed) conductance fluctuations. We would like to stress that this explanation of the characteristic frequencies in the conductance is based on transport calculations and is thus not equivalent to a rather common point of view when the observed frequencies in the conductance oscillations of an open dot are assigned to the contributions from specific periodic orbits in a corresponding closed dot [1, 2, 3, 4, 5, 6, 7, 8, 9, 11].

To conclude, we present experimental studies of the geometry-specific quantum scattering in a microwave billiard of a given shape. We perform full quantum mechanical (QM) scattering calculations and find an excellent agreement with the experimental results. We also carry out the semiclassical (SC) calculations where the conductance is given as a sum of all classical trajectories between the leads, each of them carrying the quantum-mechanical phase. Our results thus provide the first unambiguous identification of the specific frequencies of the oscillations observed in a billiard of a given shape.

Financial support from the National Graduate School in Scientific Computing (T.B) and the Swedish Research Council (I.V.Z) is acknowledged. The experiments were supported by the Deutsche Forschungsgemeinschaft.

- [1] C. Marcus et al., Phys. Rev. Lett. 69, 506 (1992).
- [2] A. M. Chang et al., Phys. Rev. Lett. **73** 2111 (1994).
- [3] M. Persson et al., Phys. Rev. B 52, 8921 (1995).
- [4] J. P. Bird et al., Europhysics Lett. 35, 529 (1996).
- [5] I. V. Zozoulenko et. al., Phys. Rev. B 55, 10 209 (1997);
   I. V. Zozoulenko and K.-F. Berggren, Phys. Rev. B 56, 6931 (1997).
- [6] R. Akis, D. K. Ferry, J. P. Bird, Phys. Rev. Lett. B 79, 123 (1997); I. V. Zozoulenko and T. Lundberg, Phys. Rev. Lett. 81, 1744 (1998).
- [7] L. Christensson et. al., Phys. Rev. B 57 12 306 (1998).
- [8] P. Bøggild et. al., Phys. Rev. B, **57** 15 408 (1998).
- [9] I. V. Zozoulenko et. al., Phys. Rev. B 58, 10594 (1998).
- [10] I. V. Zozoulenko et al., Phys. Rev. Lett. 83, 1838 (1999).
- [11] Y. Takagaki and K. H. Ploog, Phys. Rev. E 62, 4804 (2000).
- [12] For a review, see e.g., C. W. J. Beenakker, Rev. Mod. Phys. 69, 731 (1997).
- W. H. Miller, Adv. Chem. Phys. 25, 69 (1974); R. Blümel and U. Smilansky, Phys. Rev. Lett. 60, 477 (1988); R. A. Jalabert, Harold U. Baranger and A. Douglas Stone, Phys. Rev. Lett. 65, 2442 (1990).
- [14] C. D. Schwieters, J. A. Alford, and J. B. Delos, Phys. Rev. B 54, 10 652 (1996).
- [15] L. Wirtz, J.-Z. Tang and J. Burgdörfer, Phys. Rev. B 56, 7589 (1997).
- [16] T. Blomquist and I. V. Zozoulenko, Phys. Rev. B 61, 1724 (2000).
- [17] T. Blomquist and I. V. Zozoulenko, Phys. Rev. B 64, 195301 (2001).
- [18] M. C. Gutzwiller, Chaos in Classical and Quantum Mechanics (Springer-Verlag, New York, 1991).
- [19] H.-J. Stöckmann, Quantum chaos: an introduction (Cambridge University Press, Cambridge, 1999).
- [20] Y.-H. Kim et. al. Phys. Rev. B 65, (2002), in press.
- [21] A. Fuhrer et. al., Phys. Rev. B 63, 125309 (2001).
- [22] see, e.g., S. Datta, Electronic Transport in Mesoscopic Systems (Cambridge University Press, Cambridge, 1995).
- [23] I. V. Zozoulenko, F. A. Maaø and E.H. Hauge, Phys. Rev. B 53, 7975 (1996); ibid., 53, 7987 (1996); ibid., 56, 4710 (1997).
- [24] U. Kuhl et. al., Eur. Phys. J. B 17, 253 (2000).